Neutrophil AKT2 regulates heterotypic cell-cell interactions during vascular inflammation

Jing Li,[1] Kyungho Kim,[1] Eunsil Hahm,[1] Robert Molokie,[2,3,4] Nissim Hay,[5] Victor R. Gordeuk,[2,3] Xiaoping Du,[1] and Jaehyung Cho[1,6]

[1]Department of Pharmacology, [2]Section of Hematology/Oncology, and [3]Comprehensive Sickle Cell Center, University of Illinois College of Medicine, Chicago, Illinois, USA. [4]Jesse Brown VA Medical Center, Chicago, Illinois, USA. [5]Department of Biochemistry and Molecular Genetics and [6]Department of Anesthesiology, University of Illinois College of Medicine, Chicago, Illinois, USA.

Interactions between platelets, leukocytes, and activated endothelial cells are important during microvascular occlusion; however, the regulatory mechanisms of these heterotypic cell-cell interactions remain unclear. Here, using intravital microscopy to evaluate mice lacking specific isoforms of the serine/threonine kinase AKT and bone marrow chimeras, we found that hematopoietic cell–associated AKT2 is important for neutrophil adhesion and crawling and neutrophil-platelet interactions on activated endothelial cells during TNF-α–induced venular inflammation. Studies with an AKT2-specific inhibitor and cells isolated from WT and *Akt* KO mice revealed that platelet- and neutrophil-associated AKT2 regulates heterotypic neutrophil-platelet aggregation under shear conditions. In particular, neutrophil AKT2 was critical for membrane translocation of αMβ2 integrin, β2-talin1 interaction, and intracellular Ca^{2+} mobilization. We found that the basal phosphorylation levels of AKT isoforms were markedly increased in neutrophils and platelets isolated from patients with sickle cell disease (SCD), an inherited hematological disorder associated with vascular inflammation and occlusion. AKT2 inhibition reduced heterotypic aggregation of neutrophils and platelets isolated from SCD patients and diminished neutrophil adhesion and neutrophil-platelet aggregation in SCD mice, thereby improving blood flow rates. Our results provide evidence that neutrophil AKT2 regulates αMβ2 integrin function and suggest that AKT2 is important for neutrophil recruitment and neutrophil-platelet interactions under thromboinflammatory conditions such as SCD.

Introduction

Platelet-leukocyte-endothelial cell interactions can contribute to vaso-occlusion in thromboinflammatory disease (1, 2). During venular inflammation, neutrophils roll over the activated endothelium through interaction between selectins and their ligands (3). Activated neutrophil αLβ2 and αMβ2 integrins then interact with adhesion molecules such as intercellular adhesion molecule 1 (ICAM-1) on the activated endothelium, thereby regulating neutrophil adhesion and crawling, respectively (4). Importantly, activated platelets roll over and attach to adherent and crawling neutrophils during venular inflammation (5). Platelet P-selectin interacts with neutrophil P-selectin glycoprotein ligand 1 (PSGL-1), which induces the rolling of platelets over adherent neutrophils (6). Stable platelet-neutrophil interactions are mediated by the binding of platelet glycoprotein Ibα (GPIbα) to neutrophil αMβ2 integrin (7, 8). Conversely, platelets rapidly adhere to the activated endothelium or subendothelial matrix proteins such as collagen and von Willebrand factor during thrombus formation at the site of arterial injury. Adherent platelets then support neutrophil rolling and adhesion (6). Although neutrophils and platelets preferentially adhere to the activated endothelium under low- and high-shear conditions, respectively, the receptors and counter-receptors required for heterotypic cell-cell interactions are similar under both conditions (9). Despite extensive understanding of receptor-counter-receptor interactions, it remains unclear how heterotypic cell-cell interactions are regulated under thromboinflammatory conditions.

AKT is a serine/threonine kinase that participates in essential cellular processes such as cell survival, proliferation, and metabolism (10). Phosphorylation of Thr308 mediated by 3-phosphoinositide–dependent kinase 1 significantly increases AKT activity, whereas the maximal activity of AKT requires phosphorylation of Ser473, which is catalyzed by mammalian target of rapamycin complex 2 (11). AKT phosphorylates numerous substrates including glycogen synthase kinase 3β, nitric oxide synthase, and phosphodiesterase 3A (12). Despite 80% homology in protein sequences of the three known isoforms, studies with AKT isoform–specific KO mice revealed overlapping but distinct roles during platelet activation and aggregation (13–15). Interestingly, genomic studies of 500 healthy European individuals demonstrated that single nucleotide polymorphisms in the gene encoding AKT2 change platelet activity (16). In human and mouse neutrophils, only AKT1 and AKT2 are expressed, and AKT2, but not AKT1, translocates to the leading edge of neutrophils upon N-formyl-methionyl-leucyl-phenylalanine (fMLF) stimulation and regulates O_2 production through NADPH oxidase 2 (NOX2) activity (17). It was reported that endothelial cell AKT1 — a major isoform of endothelial cell AKT — is important for leukocyte recruitment during vascular leakage (18) and that AKT1 plays an important role in vascular protection against atherogenesis (19). Recent studies have shown that macrophage AKT3 plays a protective role in atherosclerosis (20). Therefore, depending on the isoform and tissue localization, AKT plays an important role in cardiovascular disease.

Here, we have explored the role of AKT during thromboinflammatory disease. Fluorescence intravital microscopic studies demonstrated that hematopoietic cell AKT2 plays a critical role during neutrophil recruitment and neutrophil-platelet interactions dur-

Conflict of interest: The authors have declared that no conflict of interest exists.
Citation for this article: *J Clin Invest.* 2014;124(4):1483–1496. doi:10.1172/JCI72305.

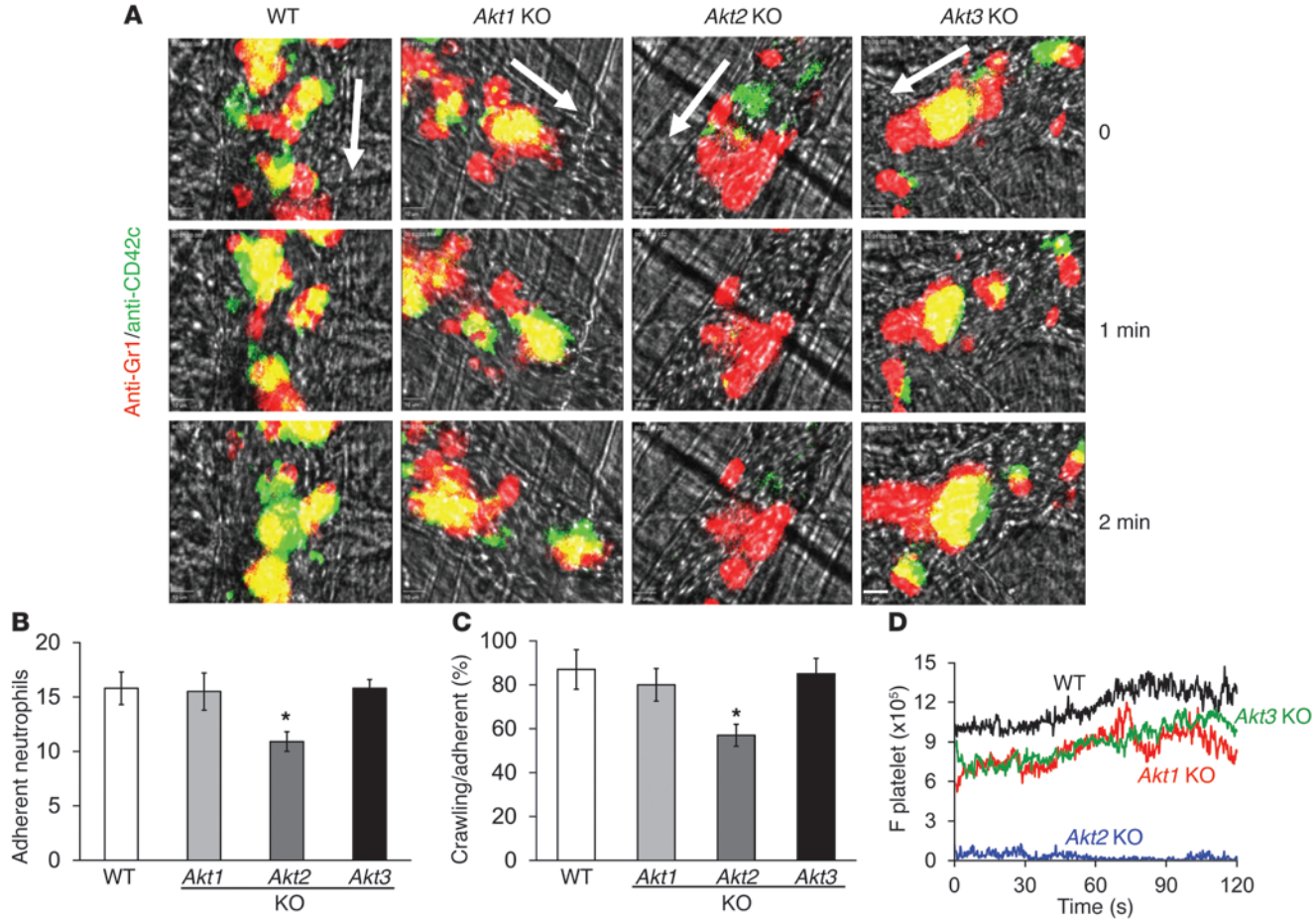

Figure 1

AKT2 is required for neutrophil recruitment and neutrophil-platelet interactions on the activated endothelium during TNF-α–induced venular inflammation. Vascular inflammation was induced by intrascrotal injection of TNF-α into WT and AKT isoform–specific KO mice. Intravital microscopy was performed as described in the Methods. Neutrophils and platelets were visualized by infusion of Alexa Fluor 647–conjugated anti-Gr1 and Dylight 488–conjugated anti-CD42c antibodies, respectively. (**A**) Representative images at various time points after monitoring. Arrows show direction of blood flow. Scale bar: 10 μm. (**B**) Number of adherent neutrophils. (**C**) Ratio of crawling/adherent neutrophils (percentage). (**D**) Median integrated fluorescence intensities of anti-CD42c antibodies (F platelets) were obtained from 45 to 52 venules, normalized by the number of adherent neutrophils, and plotted as a function of time. Data represent the mean ± SEM (n = 45–52 venules in 6 mice per group). *P < 0.05 versus WT mice by ANOVA and Dunnett's test.

ing TNF-α–induced vascular inflammation in live mice. Using in vitro reconstituted systems, we show that both platelet and neutrophil AKT2 are important for heterotypic cell-cell aggregation under shear conditions. Interestingly, neutrophil AKT2 regulated membrane translocation and activation of αMβ2 integrin. Studies of neutrophils and platelets isolated from sickle cell disease (SCD) patients and Berkeley (SCD) mice suggest that inhibition of AKT2 reduces neutrophil-platelet aggregation on the activated endothelium, thereby increasing the rate of blood flow. Thus, we provide evidence that AKT2 could be a therapeutic target for the prevention and treatment of thromboinflammatory disease.

Results

AKT2, but not AKT1 or AKT3, plays an important role in regulating neutrophil recruitment and neutrophil-platelet interactions during TNF-α–induced venular inflammation. To investigate the role of AKT isoforms during thromboinflammatory disease, we performed fluorescence intravital microscopic analysis of a mouse model of TNF-α–induced cremaster venular inflammation. Neutrophils and platelets were visualized by infusion of Alexa Fluor 647–conjugated anti-Gr1 and Dylight 488–conjugated anti-CD42c antibodies, respectively. Compared with WT and *Akt1* or *Akt3* KO mice, *Akt2* KO mice showed significantly reduced adhesion of neutrophils to the inflamed endothelium (Figure 1, A and B, and Supplemental Videos 1–4; supplemental material available online with this article; doi:10.1172/JCI72305DS1). Neutrophil crawling mediated by activated αMβ2 integrin (4) was also inhibited in the mice lacking *Akt2*, but not *Akt1* or *Akt3* (Figure 1C). Platelets bound mainly to adherent neutrophils, whereas very few platelets directly adhered to the inflamed endothelium (Figure 1A). To quantify platelet thrombi accumulating on adherent neutrophils, the integrated fluorescence signals of anti-CD42c antibodies were measured and then normalized with the number of adherent neutrophils. Notably, neutrophil-platelet interactions on the TNF-α–inflamed endothelium were abolished in *Akt2* KO mice compared with those observed in WT, *Akt1*, and *Akt3* KO mice (Figure 1D). We detected

Table 1
Analysis of *Akt2* KO mouse blood

	WBC (10^3/μl)	NE (10^3/μl)	LY (10^3/μl)	MO (10^3/μl)	RBC (10^6/μl)	PLT (10^3/μl)
WT	8.2 ± 1.7	2.0 ± 0.5	4.4 ± 1.1	0.2 ± 0.1	8.1 ± 1.1	532.1 ± 113.7
Akt2 KO	8.0 ± 2.0	1.7 ± 0.4	5.8 ± 1.3	0.1 ± 0.0	8.5 ± 0.7	602.0 ± 80.1

Blood cells from WT and *Akt2* KO mice were counted using Hemavet 950 (Drew Scientific). Data represent the mean ± SD (n = 10 mice per group). NE, neutrophils; LY, lymphocytes; MO, monocytes; PLT, platelets; RBC, red blood cells.

no fluorescence signal by control IgG (data not shown). When we measured the rate of blood flow by infusion of fluorescent microspheres into mice (21), *Akt2*, but not *Akt1* or *Akt3*, KO mice showed significant improvement in blood flow compared with that in WT mice (820 ± 190 vs. 500 ± 85 × 10^{-6} μl/s; mean ± SD, $P < 0.05$). Although a previous report showed that *Akt2* KO mice have leukocytosis (17), the number of circulating blood cells was not different between WT and *Akt2* KO mice (Table 1). These results indicate that AKT2 plays a critical role during neutrophil recruitment and neutrophil-platelet interactions on the activated endothelium during TNF-α–induced venular inflammation.

Hematopoietic cell AKT2 is important for neutrophil recruitment and neutrophil-platelet interactions during venular inflammation. Since AKT2 is expressed in both blood and endothelial cells, we further dissected the role of hematopoietic and endothelial cell AKT2 in neutrophil recruitment and heterotypic cell-cell interactions using chimeric mice generated by bone marrow transplantation in WT and *Akt2* KO mice. Compared with the transplanted WT control and endothelial cell *Akt2* KO mice, *Akt2* KO control and blood *Akt2* KO mice exhibited significantly reduced adhesion and crawling of neutrophils on the TNF-α–inflamed endothelium (Figure 2, A and B). The fluorescence signals of anti-CD42c antibodies were abolished in the control and blood *Akt2* KO mice compared with the signals in WT control and endothelial cell *Akt2* KO mice (Figure 2C). In control experiments, we found that bone marrow transplantation did not affect the number of circulating blood cells in any of the groups (data not shown). These results indicate that hematopoietic, but not endothelial cell, AKT2 regulates neutrophil recruitment and neutrophil-platelet interactions during venular inflammation.

Both neutrophil and platelet AKT2 regulate neutrophil-platelet aggregation under venous shear. It was reported that AKT inhibitor XII (AKTi XII) is a specific AKT2 inhibitor (IC_{50} = 800 nM) with high selectivity over AKT1/AKT3 (IC_{50} >10 μM) and other kinases (protein kinases A, C, and G; IC_{50} >100 μM) in in vitro kinase assays (22). To determine the specific inhibitory effect of AKTi XII on AKT2 activity in cell-based assays, we activated human neutrophils and platelets pretreated with AKTi XII with fMLF and thrombin, respectively, followed by immunoprecipitation of lysates with antibodies against phosphorylated AKT-Ser473 (p-AKT-Ser473). Immunoblotting showed that phosphorylation of all AKT isoforms markedly increased upon agonist stimulation and that treatment with 5 to 15 μM of AKTi XII significantly inhibited phosphorylation of AKT2, but not AKT1 or AKT3, in stimulated human neutrophils and platelets (Figure 3, A and B). Similar results were also obtained in mouse neutrophils and platelets (Supplemental Figure 1, A and B). In contrast, AKTi X, a structurally unrelated pan-AKT inhibitor (30 μM), abrogated phosphorylation of all AKT isoforms in stimulated human neutrophils and platelets (Supplemental Figure 2, A and B). These results suggest that AKTi XII selectively inhibits AKT2 activity in human and mouse neutrophils and platelets.

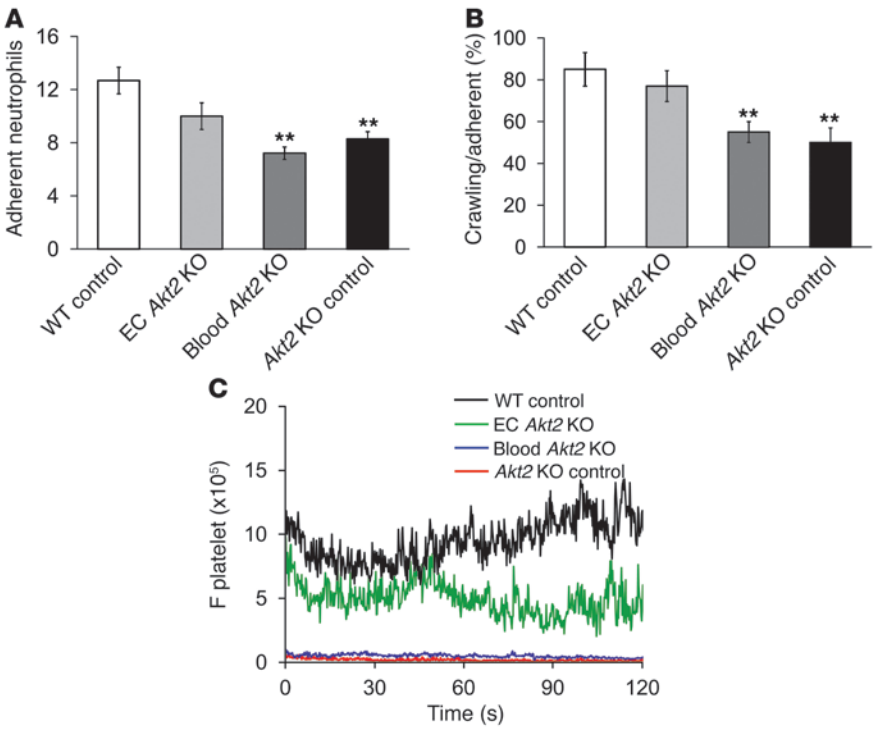

Figure 2
Hematopoietic cell AKT2 is important for neutrophil recruitment and neutrophil-platelet interactions on the TNF-α–inflamed endothelium. Chimeric mice were generated by bone marrow transplantations in WT and *Akt2* KO mice and used for intravital microscopy as described in Figure 1. (**A**) Number of adherent neutrophils. (**B**) Ratio of crawling/adherent neutrophils (percentage). (**C**) Median integrated fluorescence intensities of anti-CD42c antibodies (F platelets) were measured. Data represent the mean ± SEM (n = 60–64 venules in 8 mice per group). **$P < 0.01$ versus WT control mice by ANOVA and Dunnett's test.

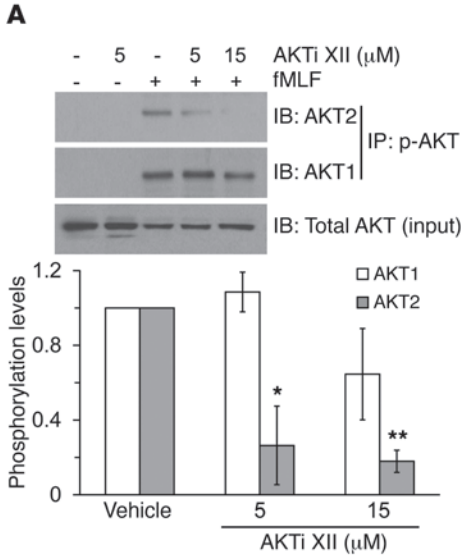
A
- 5 - 5 15 AKTi XII (μM)
- - + + + fMLF
IB: AKT2
IB: AKT1
IP: p-AKT
IB: Total AKT (input)
Phosphorylation levels
1.2
0.8
0.4
0
AKT1
AKT2
*
**
Vehicle
5
15
AKTi XII (μM)

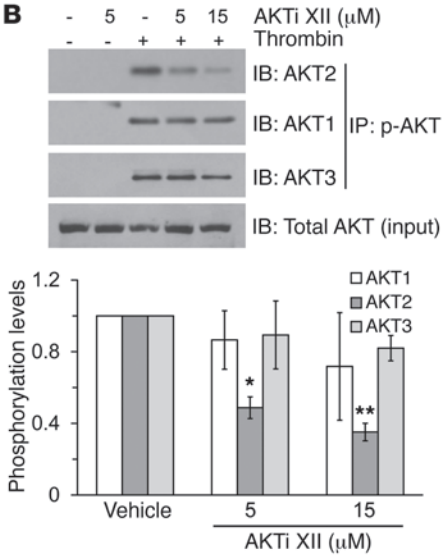
B
- 5 - 5 15 AKTi XII (μM)
- - + + + Thrombin
IB: AKT2
IB: AKT1
IB: AKT3
IP: p-AKT
IB: Total AKT (input)
Phosphorylation levels
1.2
0.8
0.4
0
AKT1
AKT2
AKT3
*
**
Vehicle
5
15
AKTi XII (μM)

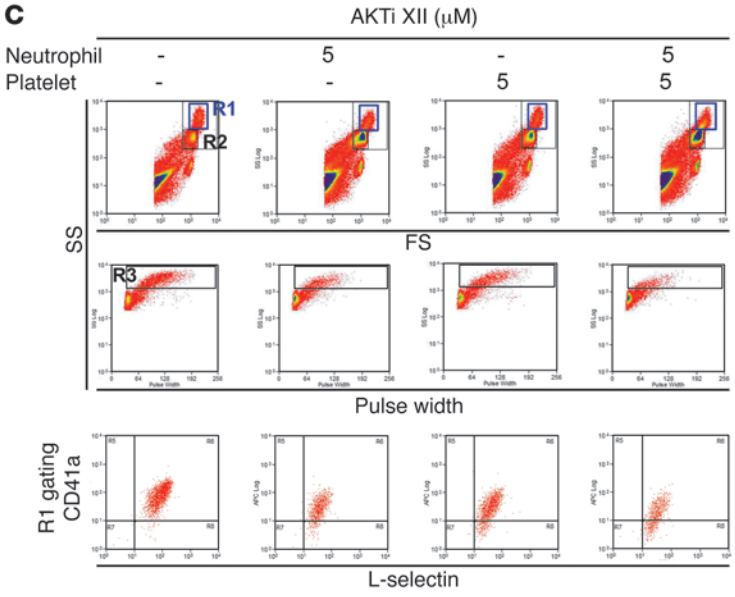
C
AKTi XII (μM)
Neutrophil - 5 - 5
Platelet - - 5 5
R1
R2
SS
FS
R3
Pulse width
R1 gating CD41a
L-selectin

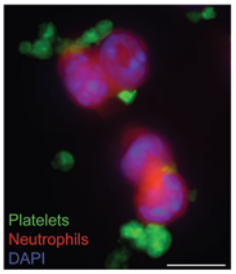
D
Platelets
Neutrophils
DAPI

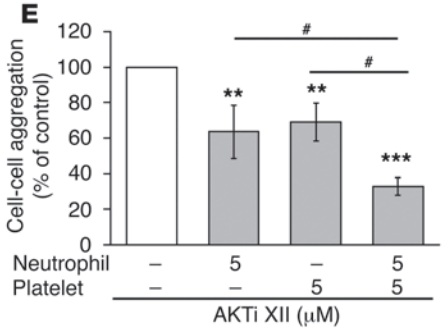
E
Cell-cell aggregation (% of control)
120
100
80
60
40
20
0
#
#
**
**
***
Neutrophil – 5 – 5
Platelet – – 5 5
AKTi XII (μM)

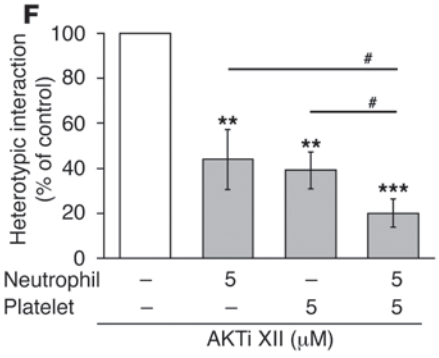
F
Heterotypic interaction (% of control)
100
80
60
40
20
0
#
#
**
**
***
Neutrophil – 5 – 5
Platelet – – 5 5
AKTi XII (μM)

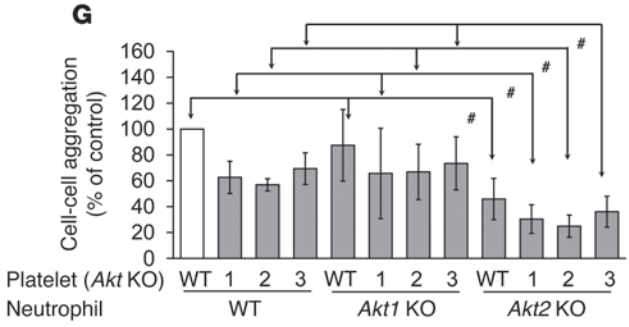
G
Cell-cell aggregation (% of control)
160
140
120
100
80
60
40
20
0
#
Platelet (Akt KO) WT 1 2 3 WT 1 2 3 WT 1 2 3
Neutrophil WT Akt1 KO Akt2 KO

Figure 3
Neutrophil and platelet AKT2 regulate heterotypic neutrophil-platelet aggregation under shear conditions. Human neutrophils (**A**) and platelets (**B**) were pretreated with 5 to 15 μM AKTi XII and stimulated with fMLF and thrombin, respectively. Lysates were immunoprecipitated with antibodies against p-AKT-Ser473, followed by immunoblotting. The band density of AKTi XII–treated groups was normalized to that of a control group (mean ± SD, $n = 3$). $^{*}P < 0.05$ and $^{**}P < 0.01$ versus control by ANOVA and Dunnett's test. (**C**–**F**) Human neutrophils and platelets were incubated with 5 μM AKTi XII and labeled with FITC-conjugated anti–L-selectin and APC-conjugated anti-CD41a antibodies, respectively. Thrombin-activated platelets were mixed with neutrophils under a stirring condition (1,000 rpm). Cells were analyzed by flow cytometry. R1, leukocyte-platelet aggregates; R2, neutrophils; and R3, number of cell aggregates in the R1 gate. Neutrophil-platelet aggregation was measured by cell-cell aggregation (R3, **E**) and the fluorescence signal of anti-CD41a antibodies (**F**) in the R1 gate. Data represent the mean ± SD ($n = 5$). $^{**}P < 0.01$ and $^{***}P < 0.001$ versus control by ANOVA and Dunnett's test, and $^{\#}P < 0.05$ by Student's *t* test. (**D**) Neutrophils and platelets were labeled with calcein red and calcein AM, respectively. After mixing both cells under a stirring condition, fluorescence microscopy was performed as described in the Methods. DAPI: blue. Scale bar: 10 μm. (**G**) Heterotypic aggregation assay was performed as described above using neutrophils and platelets isolated from WT and KO mice. Data represent the mean ± SD ($n = 4$). $^{\#}P < 0.05$ between groups by ANOVA.

Previous studies revealed that when analyzed by electron microscopy and flow cytometry (23, 24), neutrophils interact with platelets under stirring conditions (700–1,000 rpm), mimicking venous shear conditions. Using flow cytometric analysis, we sought to determine the role of neutrophil and platelet AKT2 in heterotypic neutrophil-platelet interactions. We incubated human platelets and neutrophils with APC-labeled anti-CD41a and FITC-labeled anti–L-selectin antibodies, respectively. Platelets were activated by a 2-minute incubation with 0.25 U/ml thrombin and then mixed with neutrophils under a stirring condition (1,000 rpm). We observed that a new cell population (R1 gating) appeared above a polymorphonuclear cell population (R2 gating) (Figure 3C). In the R1 gate, most cells were aggregated (Figure 3C; middle panel, R3) and were positive for both L-selectin and CD41a (Figure 3C; bottom left panel). In contrast, we found that only 26% of the cells were CD41a positive in the R2 gate. Furthermore, fluorescence microscopy with total cell aggregates showed the mixture of homotypic and heterotypic neutrophil-platelet aggregates (Figure 3D). Pretreatment of either neutrophils or platelets with 5 μM AKTi XII significantly reduced the number of neutrophil-platelet aggregates (Figure 3E) and the fluorescence signal of the anti-CD41a antibody in the R1 gate (Figure 3F). When we pretreated both cells with 5 μM AKTi XII, heterotypic aggregation was further diminished. AKTi X at 30 μM also showed similar inhibitory effects (Supplemental Figure 2C). These results indicate that both platelet and neutrophil AKT2 contribute to the regulation of heterotypic neutrophil-platelet aggregation under shear.

We further examined heterotypic aggregation of platelets and neutrophils isolated from WT and *Akt* KO mice. We incubated mouse platelets and neutrophils with Dylight 488–labeled anti-CD42c and Alexa Fluor 647–labeled anti-Gr1 antibodies, respectively. As quantified by the number of neutrophil-platelet aggregates (Figure 3G) and the fluorescence signal of the anti-CD42c antibody (data not shown), we observed moderate inhibition by incubation of WT or *Akt1* KO neutrophils with AKT isoform–specific KO platelets compared with that seen in WT platelets. *Akt2* KO neutrophils, compared with WT or *Akt1* KO neutrophils, showed further diminished heterotypic aggregation with WT or *Akt* KO platelets (Figure 3G, $^{\#}P < 0.05$). These results buttress our conclusion regarding human cells that both neutrophil and platelet AKT2 are important for heterotypic cell-cell aggregation.

Neutrophil AKT2 regulates αMβ2 integrin–mediated neutrophil-platelet interactions during venular inflammation. Previous studies showed that neutrophil αMβ2 integrin plays an important role during neutrophil recruitment and heterotypic neutrophil-platelet interactions on the activated endothelium (4, 5). We confirmed that αMβ2-null mice exhibit significant defects in neutrophil crawling and neutrophil-platelet interactions, but not in neutrophil adhesion to the activated endothelium during TNF-α–induced venular inflammation (Figure 4, A–D). Further, the blood flow rate significantly increased during venular inflammation in αMβ2-null mice compared with that in WT mice (780 ± 120 vs. 560 ± 80 × 10^{-6} μl/s; mean ± SD, $P < 0.05$). Consistent with this result, we found that inhibition or gene deletion of αM, but not αL, perturbed neutrophil-platelet aggregation and that heterotypic aggregation was further inhibited by up to 80% when αMβ2-null neutrophils were incubated with activated platelets treated with blocking anti–P-selectin antibodies (Supplemental Figure 3), supporting previous reports (9, 25) that neutrophil αMβ2 integrin and platelet P-selectin are key molecules in neutrophil-platelet interactions.

Although both αM and *Akt2* KO mice showed markedly reduced neutrophil-platelet interactions during venular inflammation, deletion of AKT2, but not the αM integrin subunit, significantly inhibited neutrophil adhesion to the inflamed endothelium (Figure 1B and Figure 4B). Thus, we further tested the effect of an anti-αMβ2 antibody and AKTi XII in *Akt2* KO and αMβ2-null mice, respectively. When we treated *Akt2* KO mice with a blocking anti-αM antibody (2 μg/g BW), no further effect was observed on neutrophil adhesion and neutrophil-platelet interactions on the TNF-α–inflamed endothelium (Figure 4, E and F). In contrast, infusion of 10 to 30 μg/g BW AKTi XII into αMβ2-null mice resulted in reduced neutrophil adhesion to the inflamed endothelium (Figure 4G). However, neutrophil-platelet interactions were not affected (Figure 4H). These results suggest that in addition to regulation of αMβ2 integrin function, AKT2 is likely to affect the function of other adhesion receptors of neutrophils, such as αLβ2 integrin. In control experiments, AKTi XII at 10 to 30 μg/g BW dose-dependently inhibited adhesion and crawling of neutrophils and neutrophil-platelet interactions on the TNF-α–inflamed endothelium in WT mice (Supplemental Figure 4, A–C). Moreover, using platelets and neutrophils isolated from WT mice treated with 10 to 30 μg/g BW AKTi XII, we demonstrated that AKTi XII specifically blocks phosphorylation of AKT2, but not AKT1 or AKT3 (Supplemental Figure 4, D and E).

AKT2 is critical for membrane translocation of αMβ2 integrin during neutrophil activation. Since P-selectin-PSGL-1 and GPIbα-αMβ2 integrin are crucial receptors-counter-receptors for neutrophil-platelet aggregation (8, 9), we determined whether the surface expression of those receptors is affected by gene deletion of AKT. In agreement with previous reports (13, 14), thrombin-activated *Akt1* and *Akt2* KO platelets exhibited partially reduced P-selectin exposure without affecting the protein expression (Figure 5, A and B). We obtained similar results with activated *Akt3* KO platelets. Consistently, pretreatment of human platelets with 5 μM AKTi XII resulted in decreased

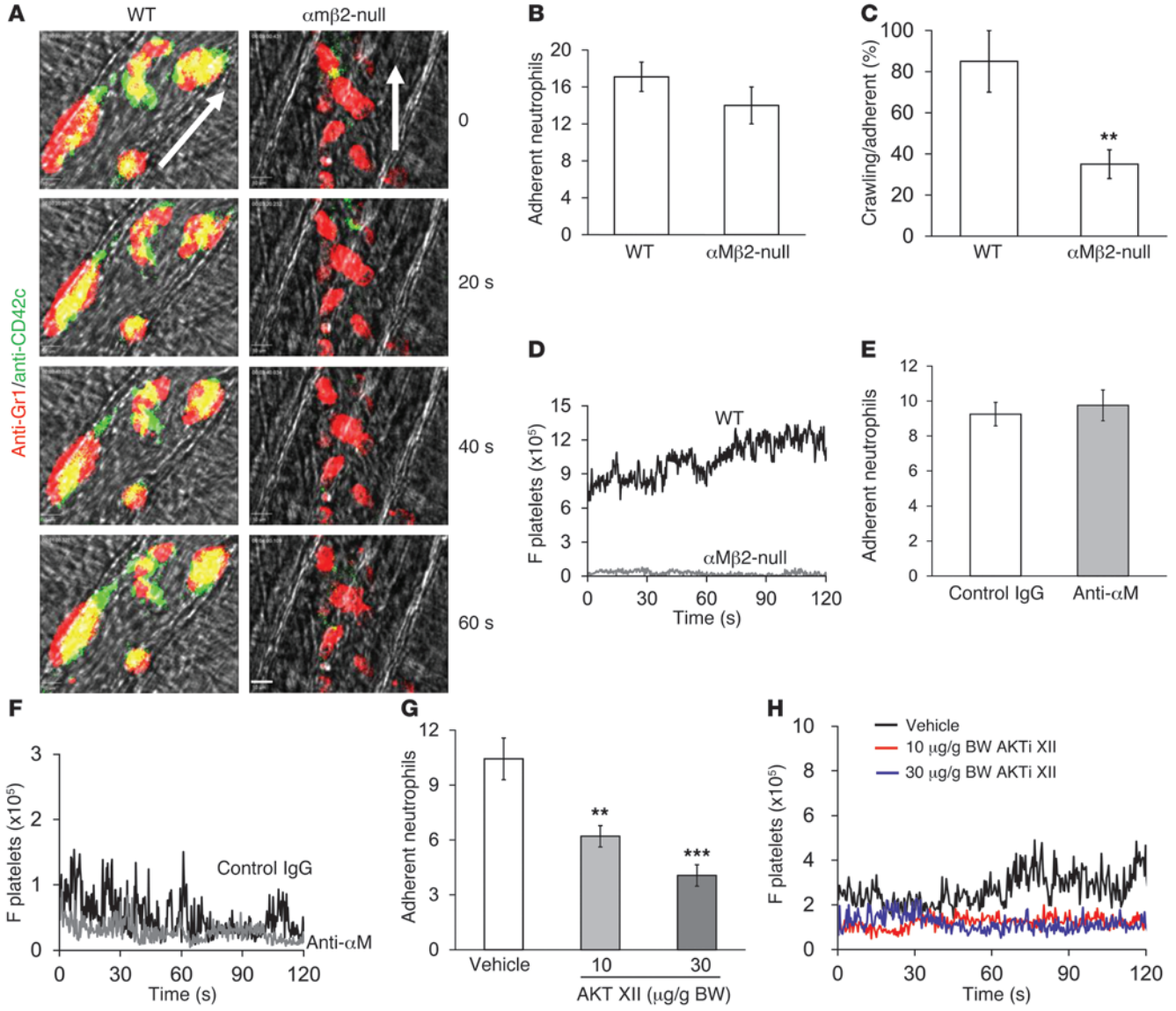

Figure 4

AKT2 regulates αMβ2 integrin–mediated neutrophil recruitment and heterotypic neutrophil-platelet interactions during TNF-α–induced venular inflammation. (**A**–**D**) Intravital microscopy of WT and αMβ2-null mice was performed as described in Figure 1. (**A**) Representative images at various time points after monitoring. Arrows show direction of blood flow. Scale bar: 10 μm. (**B**) Number of adherent neutrophils. (**C**) Ratio of crawling/adherent neutrophils (percentage). (**D**) Median integrated fluorescence intensities of anti-CD42c antibodies (F platelets). Data represent the mean ± SEM (n = 38–40 venules in 5 mice per group). $^{**}P < 0.01$ versus WT mice by Student's t test. (**E**–**H**) *Akt2* KO (**E** and **F**) or αMβ2-null mice (**G** and **H**) were treated with a blocking anti-αM antibody (2 μg/g BW) or AKTi XII (10–30 μg/g BW), respectively, 3 hours after intrascrotal injection of TNF-α. The number of adherent neutrophils (**E** and **G**) and the integrated fluorescence intensities of anti-CD42c antibodies (**F** and **H**) were measured. Data represent the mean ± SEM (n = 35–38 venules in 4 mice per group). $^{**}P < 0.01$ and $^{***}P < 0.001$ versus vehicle control by ANOVA and Dunnett's test.

P-selectin exposure upon thrombin stimulation (Figure 5C). However, WT and *Akt* KO neutrophils expressed similar levels of PSGL-1, with its partial shedding following fMLF stimulation (Figure 5D) (26). Since only *Akt2* KO mice showed a remarkable defect in neutrophil-platelet interactions during venular inflammation (Figure 1), the moderate reduction in P-selectin exposure on AKT isoform–specific KO platelets could not explain our in vivo results. Thus, we further examined the surface expression of GPIbα and αMβ2 integrin. WT and *Akt* KO platelets expressed similar levels of GPIbα (Figure 5E). It is known that the surface expression of αMβ2 integrin increases by granular secretion during neutrophil activation (27). Interestingly, we found that the surface expression of αMβ2, but not αLβ2, integrin is significantly reduced in *Akt2*, but not *Akt1*, KO neutrophils upon fMLF stimulation (Figure 5F). We observed that the expression of αM, β2, and actin was similar between WT and *Akt* KO neutrophils (Figure 5G). Consistently, pretreatment with 5 μM AKTi XII diminished binding of antibodies against

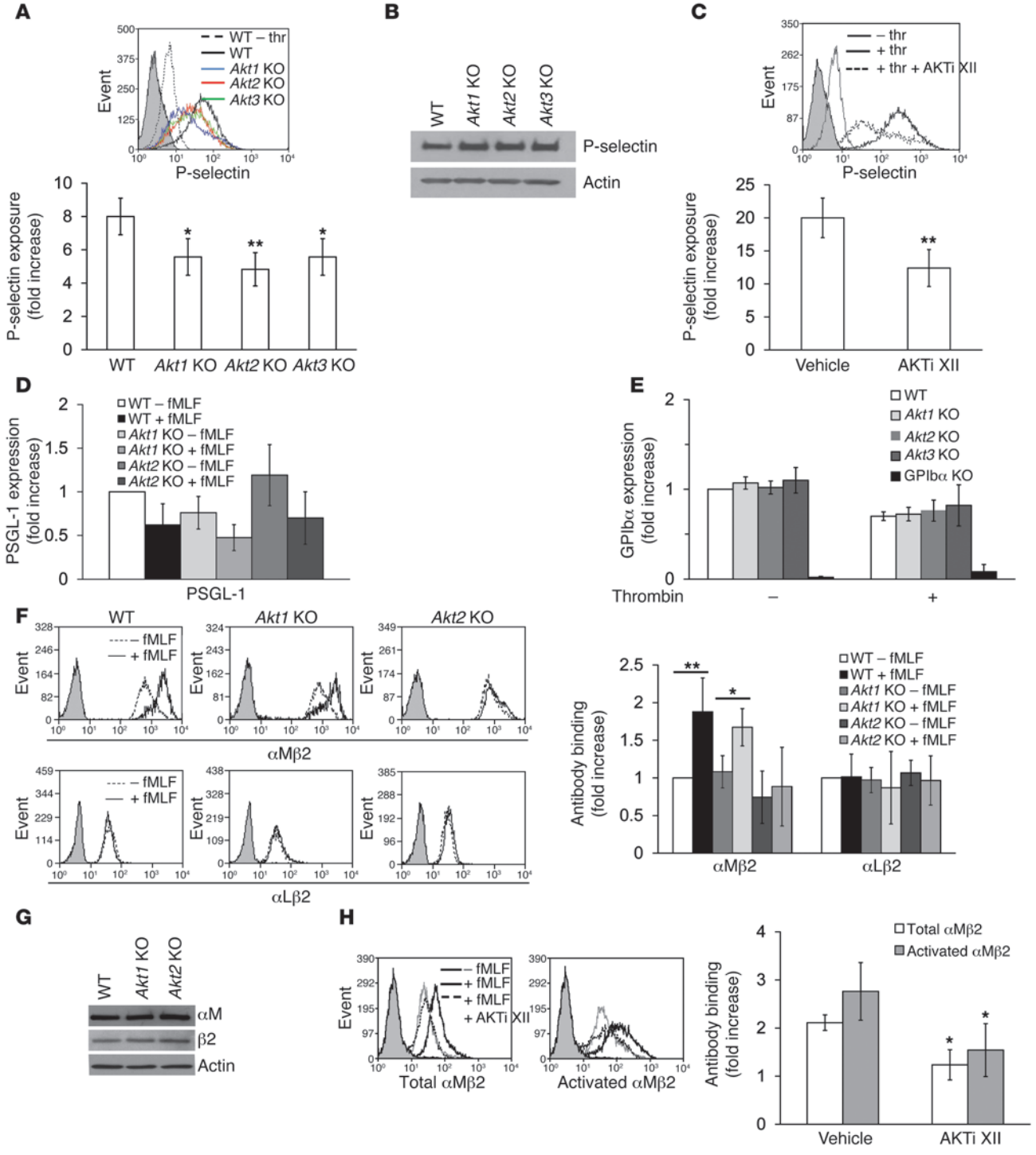

Figure 5

Effect of deletion and inhibition of AKT on the expression of platelet and neutrophil surface molecules. (**A** and **C**) Flow cytometric analysis was performed to determine P-selectin exposure on WT and *Akt* KO platelets or on human platelets treated with 5 μM AKTi XII following thrombin (thr) stimulation as described in the Methods. **P* < 0.05 and ***P* < 0.01 versus WT or vehicle control by ANOVA and Dunnett's test (**A**) or Student's *t* test (**C**). (**B**) Representative blot of P-selectin expression in lysates of WT and *Akt* KO platelets. (**D**) WT and *Akt* KO neutrophils were treated with or without fMLF and analyzed by flow cytometry using anti–PSGL-1 antibodies. (**E**) GPIbα expression was analyzed by flow cytometry using WT and *Akt* KO platelets treated with or without thrombin. (**F**) Surface expression of αMβ2 and αLβ2 integrins on unstimulated and fMLF-stimulated WT and *Akt* KO neutrophils. **P* < 0.05 and ***P* < 0.01 versus unstimulated cells by Student's *t* test. (**G**) Representative blot of αM, β2, and actin in lysates of WT and *Akt* KO neutrophils. (**H**) Human neutrophils pretreated with 5 μM AKTi XII were stimulated with fMLF. Flow cytometric analysis was performed using antibodies against total (ICRF44) and activated αMβ2 (CBRM1/5). **P* < 0.05 versus vehicle by Student's *t* test. All data were obtained from four independent experiments (mean ± SD).

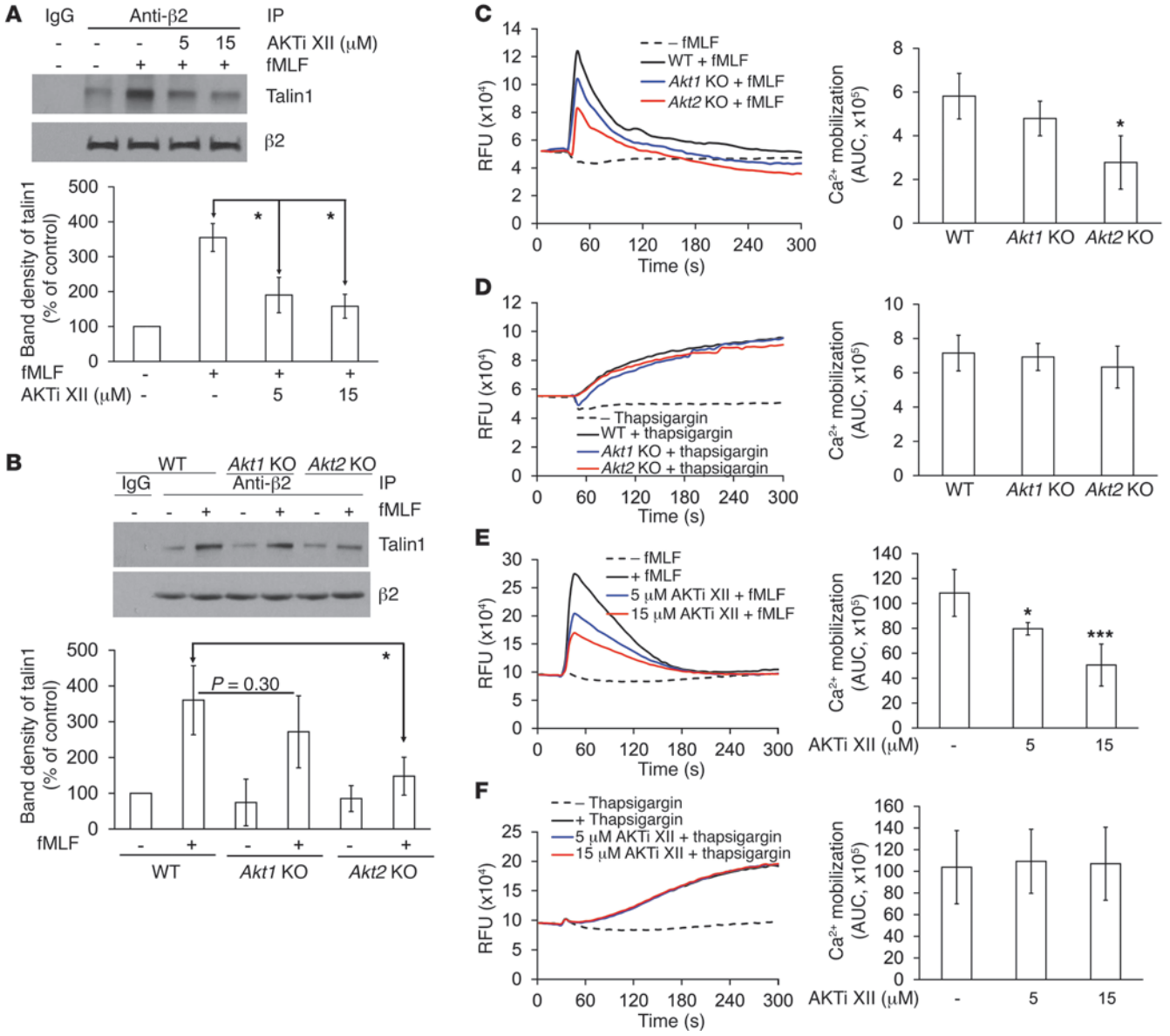

Figure 6

AKT2 regulates β2-talin1 interaction and intracellular Ca^{2+} mobilization during neutrophil activation. (**A** and **B**) Human neutrophils treated with 5 to 15 μM AKTi XII or neutrophils isolated from WT and *Akt* KO mice were incubated with or without fMLF for 1 minute. Lysates were immunoprecipitated with antibodies against β2 and immunoblotted. (**C**–**F**) Neutrophils isolated from WT and *Akt* KO mice or human neutrophils treated with 5 to 15 μM AKTi XII were preincubated with a Ca^{2+} dye and then treated with or without fMLF or thapsigargin in the absence of extracellular Ca^{2+}. Intracellular Ca^{2+} mobilization was measured and quantified by AUC (× 10^5 arbitrary units). All data were obtained from four independent experiments and represent the mean ± SD. **P* < 0.05 and ****P* < 0.001 versus WT or vehicle control by Student's *t* test (**B**) or ANOVA and Dunnett's test. RFU, relative fluorescence units.

total (ICRF44) or activated (CBRM1/5) human αMβ2 integrin to fMLF-stimulated human neutrophils (Figure 5H). These results suggest that AKT2 regulates membrane translocation of αMβ2 integrin during neutrophil activation.

AKT2 regulates β2-talin1 interaction and intracellular Ca^{2+} mobilization during neutrophil activation. Although the reduced surface expression of αMβ2 integrin will affect CBRM1/5 binding to human neutrophils (Figure 5H), we could not rule out the possibility that AKT2 modulates integrin activation through inside-out signaling. Binding of talin to the cytoplasmic tail of the β integrin subunit is essential for inside-out signaling–mediated integrin activation (28). Thus, we investigated whether AKT2 regulates the β2-talin1 interaction following agonist stimulation. Lysates of unstimulated and fMLF-stimulated human and mouse neutrophils were coimmunoprecipitated with anti-β2 antibodies, followed by immunoblotting with anti-talin1 antibodies. We found that the β2-talin1 interaction increased upon fMLF stimulation and that the increased interaction was significantly inhibited by pretreatment with 5 to 15 μM AKTi XII (Figure 6A). Further, *Akt2* KO neutrophils, compared with WT and *Akt1* KO neutrophils, showed a

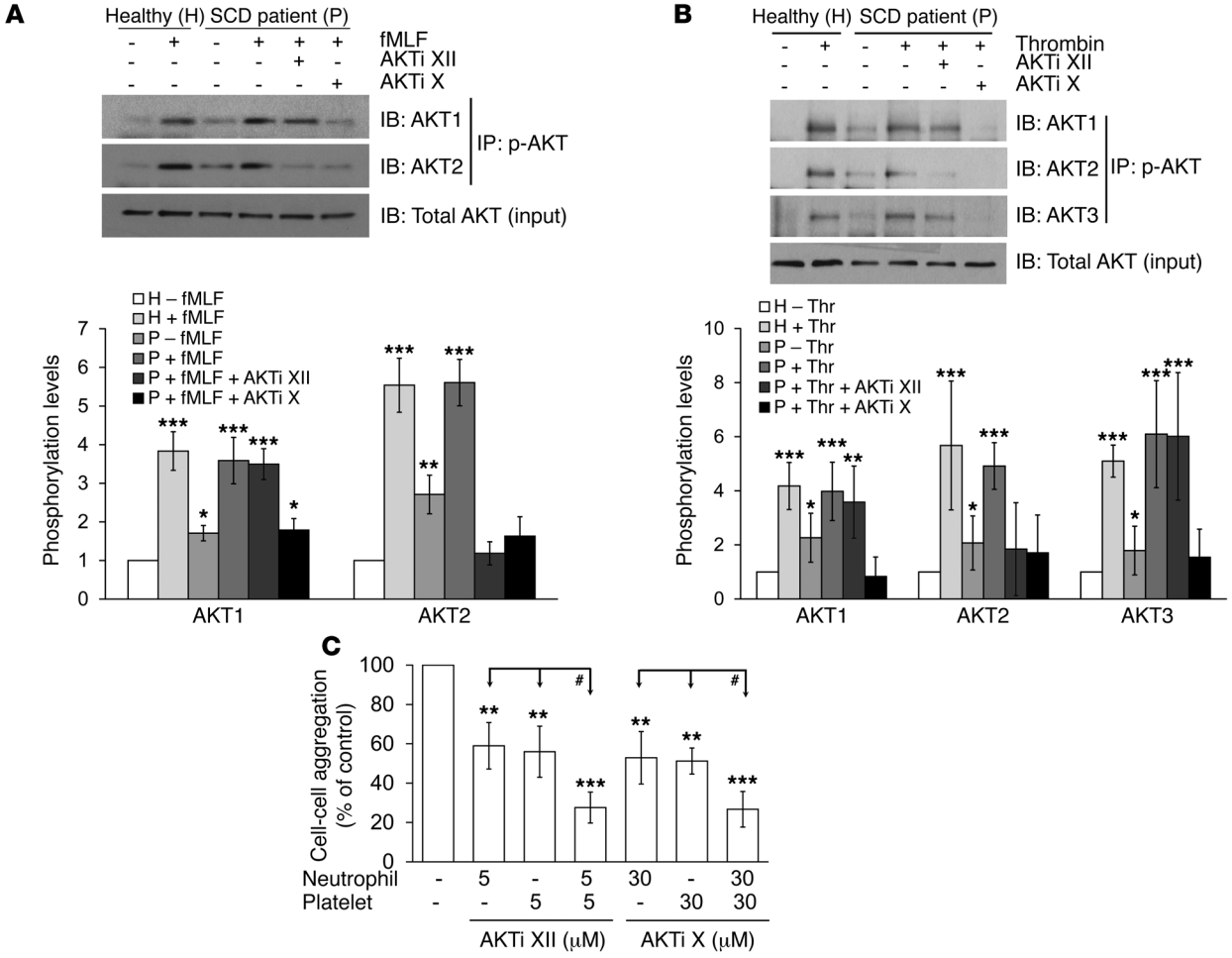

Figure 7

AKT2 regulates in vitro heterotypic aggregation of neutrophils and platelets isolated from SCD patients. Neutrophils (**A**) and platelets (**B**) of SCD patients were pretreated with or without 5 μM AKTi XII or 30 μM AKTi X and then stimulated with fMLF and thrombin, respectively. Lysates were immunoprecipitated with antibodies against p-AKT-Ser473 and immunoblotted. Band density represents the mean ± SD (n = 6 patients per group). *P < 0.05, **P < 0.01, and ***P < 0.001 versus unstimulated healthy donor by ANOVA and Dunnett's test. (**C**) Neutrophils and platelets from patients were pretreated with 5 μM AKTi XII or 30 μM AKTi X and used for the in vitro aggregation assay described in Figure 3. Heterotypic aggregation was quantified by cell-cell aggregation. Data represent the mean ± SD (n = 8 patients). **P < 0.01 and ***P < 0.001 versus vehicle control by ANOVA and Dunnett's test, and #P < 0.05 by ANOVA.

significant reduction in the β2-talin1 interaction (Figure 6B). These results indicate that in addition to the quantitative regulation of αMβ2 integrin, neutrophil AKT2 is critical for inside-out signaling–mediated activation of β2 integrins.

Previous studies have suggested that AKT could regulate Ca^{2+} signaling in cardiomyocytes (29). Since Ca^{2+} is a critical second messenger for numerous cellular functions including exocytosis and integrin function, we studied whether AKT2 regulates intracellular Ca^{2+} mobilization during neutrophil activation. Compared with WT neutrophils, *Akt2* KO neutrophils significantly inhibited intracellular Ca^{2+} mobilization, whereas *Akt1* KO neutrophils showed a minimal defect (Figure 6C). However, gene deletion of AKT2 did not affect persistent intracellular Ca^{2+} pool depletion induced by thapsigargin, an inhibitor of endoplasmic reticulum Ca^{2+}-ATPase (Figure 6D). Further, we obtained similar results by treating human neutrophils with 5 to 15 μM AKTi XII (Figure 6, E and F). Thus, these results indicate that AKT2 plays an important role in regulating intracellular Ca^{2+} mobilization without affecting the amount of intracellular Ca^{2+}.

AKT2 regulates in vitro heterotypic aggregation of neutrophils and platelets of SCD patients as well as neutrophil adhesion and neutrophil-platelet interactions in venules of SCD mice. Heterotypic platelet-leukocyte-sickle red cell interactions occurring on the activated endothelium can induce vaso-occlusion in SCD patients, causing pain crisis and organ failure (30). Since our results have shown that AKT2 regulates heterotypic cell-cell interactions during venular inflammation, we investigated whether AKT activity is changed in the platelets and neutrophils of homozygous SCD patients. Intriguingly, the basal phosphorylation level of AKT isoforms was enhanced by approximately 2- to 3-fold in lysates of neutrophils and platelets from patients (Figure 7, A and B). However, we observed no difference in AKT phosphorylation levels between healthy donors' and patients' cells following agonist stimulation. Pretreatment of patients' neutrophils and platelets with 5 μM

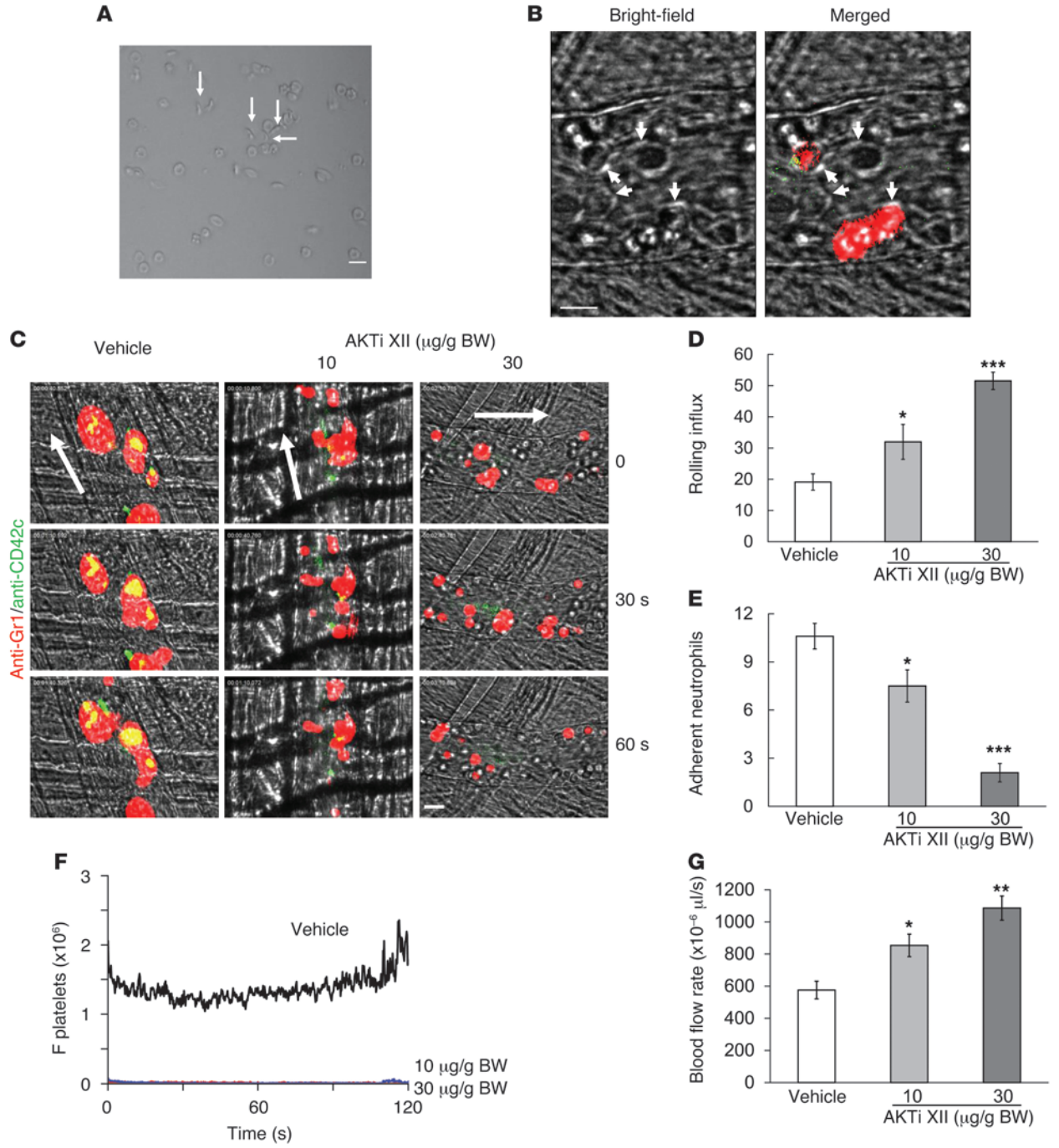

Figure 8

AKTi XII dose-dependently inhibits heterotypic cell-cell interactions in venules of Berkeley mice. (**A**) Smears of Berkeley mouse blood were observed under a microscope ($n = 4$). Arrows show sickle red cells. Scale bar: 10 μm. (**B**–**E**) Berkeley mice were treated with vehicle or 10 or 30 μg/g BW AKTi XII, and intravital microscopy was performed without intrascrotal injection of TNF-α, as described in the Methods. (**B**) Sickle red cells attached to adherent neutrophils (Gr1-positive, red) and other leukocytes (Gr1-negative) in Berkeley mice. Green indicates platelet(s). (**C**) Representative images at various time points after monitoring. Arrows show direction of blood flow. Scale bar: 10 μm. Number of rolling (**D**) and adherent neutrophils (**E**). (**F**) Median fluorescence intensities of anti-CD42c antibodies (F platelets). (**G**) Blood flow rates were measured as described in the Methods. Data represent the mean ± SEM ($n = 48$–52 venules in 6 mice). $^*P < 0.05$, $^{**}P < 0.01$, and $^{***}P < 0.001$ versus vehicle control by ANOVA and Dunnett's test.

AKTi XII reduced phosphorylation of only AKT2 to the basal level of healthy donors' cells, whereas pretreatment with 30 μM AKTi X abolished phosphorylation of all AKT isoforms (Figure 7, A and B). When either neutrophils or platelets of patients were pretreated with 5 μM AKTi XII or 30 μM AKTi X, we found that neutrophil-platelet aggregation was inhibited by 45% compared with that observed in controls (Figure 7C). Treatment of both cell types with the inhibitors further reduced neutrophil-platelet aggrega-

tion by 70% compared with controls, suggesting that AKT2 could be a dominant AKT isoform controlling heterotypic aggregation of neutrophils and platelets in SCD patients.

To examine whether inhibition of AKT2 alleviates neutrophil adhesion and neutrophil-platelet interactions on the venular endothelium in SCD, we performed intravital microscopy studies of Berkeley mice. Consistent with a previous report (31), 20%–30% of sickle cells were observed in smears of Berkeley mouse blood (Figure 8A). Further, we visualized adherent sickle red cells on adherent neutrophils and other leukocytes, some of which interacted with platelet(s) (Figure 8B). When we treated the mice with 10–30 μg/g BW AKTi XII, the number of rolling neutrophils was increased, whereas neutrophil adhesion was inhibited dose dependently (Figure 8, C–E). Neutrophil-platelet interactions on the endothelium were abolished even at 10 μg/g BW of AKTi XII (Figure 8F), a dose at which neutrophil adhesion was partially reduced but still retained (Figure 8E). Treatment of Berkeley mice with AKTi XII dose-dependently increased the rate of blood flow compared with that in vehicle controls (Figure 8G). We further investigated whether AKTi XII inhibits cell-cell aggregation in Berkeley mice under inflammatory conditions. Three hours after i.p. injection of TNF-α into Berkeley mice, we exposed the cremaster muscle, and 10 or 30 μg/g BW AKTi XII was infused into the mice. Treatment with AKTi XII dose-dependently increased the rolling influx of neutrophils and decreased the number of adherent neutrophils in the venules of TNF-α–challenged Berkeley mice (Supplemental Figure 5, A and B). Further, we found that neutrophil-platelet aggregation was markedly reduced after treatment with AKTi XII, even at a dose of 10 μg/g BW (Supplemental Figure 5C). Thus, our results provide important evidence that inhibition of AKT2 could protect heterotypic cell-cell aggregations in SCD under inflammatory conditions.

Discussion

Interaction of activated platelets and leukocytes on the activated vascular endothelium has been recognized as a critical determinant of thromboinflammatory disease (1, 2). In the present study, we have demonstrated that AKT2 plays a critical role in regulating stable adhesion and crawling of neutrophils and heterotypic neutrophil-platelet interactions during TNF-α–induced venular inflammation. Such regulatory effects resulted from controlling the surface expression of αMβ2 integrin, β2-talin1 interaction, and intracellular Ca^{2+} mobilization during neutrophil activation. Furthermore, inhibition of AKT2 markedly reduced neutrophil adhesion and neutrophil-platelet aggregation in the venules of Berkeley mice, thereby increasing blood flow. Thus, our results suggest that AKT2 could be a novel therapeutic target for the prevention and treatment of thromboinflammatory disease.

In addition to its localization on the plasma membrane, αMβ2 integrin is stored in three different secretory granules of unstimulated neutrophils: — specific (secondary) and tertiary granules and secretory vesicles — and translocates to the plasma membrane upon agonist stimulation (32). Previous studies showed that release of β-glucuronidase from azurophilic (primary) granules is substantially inhibited in *Akt2* KO neutrophils following fMLF stimulation (17). Further, Nanamori et al. reported that protein kinase G and phosphatidylinositol-3-kinase regulate granular exocytosis in rat mast cells, probably through phosphorylation of soluble N-ethylmaleimide–sensitive factor attachment protein receptor (33). Using an AKT2-specific inhibitor, AKTi XII, and *Akt* KO neutrophils, we found that neutrophil AKT2, but not AKT1, is critical for membrane translocation of αMβ2 integrin upon fMLF stimulation. Although it remains to be determined how AKT2 modulates granular exocytosis during cell activation, these results indicate that AKT2 is a key regulator of exocytosis of all neutrophil granules. The functional disparity between AKT1 and AKT2 could be due to their different subcellular localization following agonist stimulation; AKT2 rapidly localizes to the leading edge, whereas AKT1 remains in cytoplasmic regions (17, 34).

Heterotypic leukocyte-platelet interactions are initiated by binding of platelet P-selectin to leukocyte PSGL-1 (25). P-selectin-PSGL-1 interaction subsequently induces another interaction between GPIbα and activated αMβ2 integrin, thereby resulting in stable leukocyte-platelet attachment (8). Although neutrophil-platelet aggregation under venous shear was moderately reduced by AKT isoform–specific KO platelets, probably due to the reduced P-selectin exposure (Figure 5A), our intravital microscopic analysis clearly demonstrated that only AKT2 plays a critical role during neutrophil recruitment and neutrophil-platelet interactions on the inflamed endothelium, thereby regulating blood flow. Thus, our results suggest that partial inhibition of P-selectin alone do not inhibit heterotypic neutrophil-platelet interactions and vaso-occlusion during vascular inflammation and that the abolished neutrophil-platelet interactions in *Akt2* KO mice result from inhibition of neutrophil αMβ2 integrin function combined with decreased P-selectin exposure. It was thought that platelet αIIbβ3 integrin may be important for the interaction with neutrophil αMβ2 integrin through fibrinogen (9). However, consistent with previous reports (35, 36), we found that integrilin, an αIIbβ3 integrin antagonist, slightly potentiates neutrophil-platelet aggregations under shear (Supplemental Figure 3). More recently, Kleinschnitz and colleagues reported that F(ab′)2 fragments against αIIbβ3 integrin have no inhibitory effect on stroke size, but increase the incidence of intracerebral hemorrhage after transient middle cerebral artery occlusion in mice (37). Moreover, clinical studies in patients with ischemic stroke demonstrated that inhibition of αIIbβ3 integrin with abciximab or tirofiban results in fatal intracerebral hemorrhage (38, 39).

We found that unlike αMβ2-null mice, *Akt2* KO mice showed a significant defect in neutrophil adhesion, suggesting that AKT2 may regulate the function of other adhesion receptors such as αLβ2 integrin. This speculation is supported by our findings that AKT2 is a critical regulator of β2-talin1 interaction and intracellular Ca^{2+} mobilization, which control the activation and function of β2 integrins. Conformational change and clustering of αMβ2 integrin have been postulated as key mechanisms regulating its ligand-binding activity and adhesiveness (40, 41). Moser et al. reported that gene deletion of kindlin-3 in mouse leukocytes results in functional defects in β2 integrin–dependent leukocyte adhesion, thereby causing a leukocyte adhesion deficiency type III–like phenotype (42). Interaction of the β2 cytoplasmic tail with talin1 is believed to be a final step in integrin activation and controls the ligand-binding activity of the integrin (28, 43). We observed that inhibition and gene deletion of AKT2 significantly inhibit β2-talin1 interaction. Although further studies are required to elucidate how AKT2 regulates binding of talin1 to the β2 cytoplasmic tail, our results demonstrate that AKT2 is required for β2 integrin activation following agonist stimulation. Previous studies showed that AKT plays a positive or negative role in Ca^{2+} signaling. AKT is important for the function of the L-type Ca^{2+}

channel in cardiac myocytes of type 2 diabetic mice (29), whereas overexpression of constitutively active AKT1 in HeLa cells reduces Ca^{2+} release from the endoplasmic reticulum following agonist stimulation (44). Our studies with AKTi XII and *Akt2* KO neutrophils revealed that AKT2 positively regulates Ca^{2+} mobilization during neutrophil activation. Since the function of key players in Ca^{2+} signaling, including inositol 1,4,5-triphosphate receptor, could be modulated by protein phosphorylation (45), AKT2 may phosphorylate serine/threonine residues on those molecules, thereby regulating their function during neutrophil activation.

Recurrent vascular occlusion is known to increase morbidity and mortality in SCD patients due to organ damage, vascular inflammation, and cerebrovascular injury (30). Vaso-occlusion induced by sickle red cell-leukocyte-platelet-endothelial cell heterotypic aggregation was abrogated by treatment with a selectin inhibitor in Berkeley mice (46). We found that AKT phosphorylation was significantly elevated in unstimulated neutrophils and platelets of SCD patients and that inhibition of AKT2 blocked heterotypic neutrophil-platelet aggregation (Figure 7, A–C). We also observed that neutrophils and platelets of SCD patients showed increased αMβ2 integrin activation and P-selectin exposure, respectively, in the absence of an agonist compared with cells from healthy donors, suggesting that patients' blood cells are partially activated (Supplemental Figure 6). Interestingly, compared with *Akt2* KO mice during TNF-α–induced venular inflammation, treatment of Berkeley mice with 30 μg/g BW AKTi XII inhibited neutrophil adhesion to the activated endothelium by greater than 80%. These results could be derived from the relatively weak inflammatory conditions in Berkeley mice, since the number of rolling neutrophils was greater in these mice (19.1 ± 2.4 cells/min) than in WT mice intrascrotally injected with TNF-α (0.3 ± 0.1 cells/min). Indeed, the rolling influx of neutrophils was markedly decreased when Berkeley mice were challenged by i.p. injection of TNF-α (1.9 ± 0.4 neutrophils/min), indicating that the Berkeley mice were not under strong inflammatory conditions. It should be noted that neutrophil adhesion was still retained after treatment with 10 μg/g BW AKTi XII, a dose at which neutrophil-platelet interactions were abolished and blood flow rates were significantly improved (Figure 8). These results show that in addition to adherent neutrophils, neutrophil-platelet interactions could play an important role during microvascular occlusion in SCD. Further, our results provide important evidence that inhibition of AKT2 may be effective in the treatment of vaso-occlusion in SCD patients under inflammatory conditions.

It was reported that *Akt2* gene deletion causes hyperinsulinemia and diabetes mellitus–like syndrome, since it is highly expressed in insulin-responsive tissues (47). Interestingly, diabetes induced by deletion of *Akt2* could be reversed by leptin therapy, whereby leptin was restored in *Akt2* KO mice (48). Although we did not see any change in blood glucose and serum insulin levels after a one-time injection of AKTi XII at a dose of 10 to 30 μg/g BW (data not shown), future studies, such as those involving long-term treatment with high concentrations of AKTi XII, are required to assess the potential side effects of targeting AKT2. Additionally, we cannot rule out the possibility that additional signaling pathways independent of AKT2 could be involved in regulating cellular functions during deletion and inhibition of AKT2. Taken together, our studies indicate that neutrophil AKT2 regulates membrane translocation and activation of αMβ2 integrin, thereby playing an important role in neutrophil recruitment and neutrophil-platelet interactions under thromboinflammatory conditions. Since previous studies demonstrated that leukocyte-platelet interactions increase in patients experiencing clinical events including restenosis, myocardial infarction, and unstable angina after coronary angioplasty (49), our results provide important genetic and pharmacologic evidence that AKT2 may be a novel therapeutic target for the prevention and treatment of thromboinflammatory disease.

Methods

Mice. Six- to 8-week-old WT (C57BL/6), αM (*Itgam*) KO, αL (*Itgal*) KO, and Berkeley mice were purchased from The Jackson Laboratory. *Akt1*, *Akt2*, *Akt3*, and GPIbα (*Gp1ba*) KO mice on a C57BL/6 background were described previously (48, 50–52). Age-matched (6- to 10-week-old) male mice were used in our studies.

Bone marrow transplantation, flow cytometric analysis, immunoprecipitation, and calcium mobilization. Detailed methods are described in the Supplemental Methods.

Isolation of human and mouse neutrophils and platelets. Neutrophils in human blood and mouse bone marrow were isolated as described previously (40). The isolation of human and mouse platelets and SCD patient information are described in the Supplemental Methods. Human and mouse neutrophils were stimulated for 10 minutes at 37°C with 0.5 and 10 μM fMLF, respectively, unless otherwise stated.

In vitro neutrophil-platelet aggregation. Human platelets and/or neutrophils were incubated with AKT inhibitors for 45 minutes at 37°C and washed, followed by labeling with APC-conjugated anti-human CD41a and FITC-conjugated anti–L-selectin antibodies, respectively. Platelets were treated with 0.25 U/ml thrombin at room temperature for 2 minutes and then incubated with 50 μM D-phenylalanyl-L-prolyl-L-arginine chloromethyl ketone (PPACK). Activated platelets were mixed with neutrophils under a stirring condition of 1,000 rpm in an aggregometer (Chrono-log). After a 5-minute incubation, cells were fixed with 1% PFA, and samples were analyzed by flow cytometry. In some experiments, mouse platelets and neutrophils were labeled with Dylight 488–conjugated anti-mouse CD42c and Alexa Fluor 647–conjugated anti-Gr1 antibodies, respectively. Platelets were activated and then mixed with neutrophils under a stirring condition as described above, followed by flow cytometric analysis. To visualize neutrophil-platelet aggregation by fluorescence microscopy, neutrophils and platelets were labeled with 5 μg/ml calcein red and calcein AM, respectively, for 15 minutes at 37°C. After washing, heterotypic aggregation was performed as described above. Cell aggregates were fixed and attached to a glass slide by cytospin centrifugation for 5 minutes. Slides were mounted with media containing DAPI (Vector laboratories), and fluorescence images were captured with a Nikon microscope (ECLIPSE Ti) equipped with a Plan Fluor ×100/1.30NA oil objective lens and recorded with a digital camera (CoolSNAP ES2). The data were analyzed using NIS-Elements (AR 3.2; Nikon).

Fluorescence intravital microscopy in vivo. Six- to 10-week-old male mice were used for fluorescence intravital microscopy as described previously (40, 53). In some experiments,14- to 16-week-old bone marrow chimera were used. WT and KO mice were intrascrotally injected with murine TNF-α (0.5 μg). Three hours after TNF-α injection, the mouse was anesthetized by i.p. injection of ketamine and xylazine, and the cremaster muscle was exteriorized. Neutrophils and platelets were monitored by labeling of Alexa Fluor 647–conjugated anti-Gr1 (0.05 μg/g BW) and Dylight 488–conjugated anti-CD42c antibodies (0.1 μg/g BW) through a jugular vein cannula. In some experiments, Berkeley mice were treated with or without i.p. injection of TNF-α (0.5 μg). For nontreated Berkeley mice, AKTi XII was infused through a jugular cannulus 5 minutes prior to infusion of anti-Gr1 and

anti-CD42c antibodies. For TNF-α–challenged Berkeley mice, AKTi XII and anti-Gr1 and anti-CD42c antibodies were infused 3 hours after TNF-α injection. Fluorescence and bright-field images were recorded using an Olympus BX61W microscope with a 60× 1.0 NA water immersion objective and a Hamamatsu C9300 high-speed camera through an intensifier (Video Scope International), and data were analyzed using Slidebook, version 5.5 (Intelligent Imaging Innovations). Real-time images were obtained in the top half of the inflamed cremaster venules with a diameter of 25–40 μm, since smaller venules were often occluded before or during imaging. The rolling influx of neutrophils (rolling cells/minute) and the percentage of crawling neutrophils were determined over a 5-minute period in a 0.02-mm^2 area. Neutrophils with a displacement of greater than 10 μm during 1 minute were considered crawling (40). The number of adherent neutrophils that were stationary for more than 30 seconds and crawled but did not roll over were counted (number/field/5 minutes). The number of rolling and adherent neutrophils was normalized for the circulating neutrophil count. Eight to ten different venules were monitored in one mouse. To determine the kinetics of platelet accumulation, the integrated median fluorescence intensity of the anti-CD42c antibody was normalized by the number of adherent neutrophils and plotted as a function of time. To measure the rate of blood flow in venules with a diameter of 25 to 40 μm, yellow-green fluorescent microspheres (0.1-μm) were infused into mice. Centerline velocity (Vc) of the microspheres was calculated as a distance per time in the center of the venules. Blood-flow rates were calculated as $Q = Vc \times (\text{a radius of each venule})^2 \times \pi$ and are expressed as 10^{-6} μl/s.

Statistics. Data analysis was performed using GraphPad Prism 5 software (GraphPad Software). Statistical significance was assessed by ANOVA and the Dunnett's test for comparison of multiple groups or by a 2-tailed Student's *t* test for comparison of two groups. A *P* value less than 0.05 was considered statistically significant.

Study approval. All mice were treated in accordance with the guidelines for the care and use of laboratory animals under animal protocol 12-140 approved by the IACUC of the University of Illinois-Chicago. All healthy donors and patients enrolled in this study provided informed consent. The collection and use of blood samples for laboratory analysis were approved by the IRB of the University of Illinois-Chicago under protocol 2009-0812.

Acknowledgments

This work was supported in part by grants from the NIH (P30HL101302 and R01HL109439, to J. Cho; AG016927 and CA090764, to N. Hay; and HL080264 and HL062350, to X. Du) and by a University of Illinois at Chicago Center for Clinical and Translational Science Award (CCTS0413, to J. Cho).

Received for publication July 31, 2013, and accepted in revised form December 17, 2013.

Address correspondence to: Jaehyung Cho, 835 South Wolcott Avenue, E403, Chicago, Illinois 60612, USA. Phone: 312.355.5923; Fax: 312.996.1225; E-mail: thromres@uic.edu.

1. Wagner DD, Frenette PS. The vessel wall and its interactions. *Blood*. 2008;111(11):5271–5281.
2. Nieswandt B, Kleinschnitz C, Stoll G. Ischaemic stroke: a thrombo-inflammatory disease? *J Physiol*. 2011;589(pt 17):4115–4123.
3. Zarbock A, Ley K. Neutrophil adhesion and activation under flow. *Microcirculation*. 2009;16(1):31–42.
4. Phillipson M, Kubes P. The neutrophil in vascular inflammation. *Nat Med*. 2011;17(11):1381–1390.
5. Hidalgo A, Chang J, Jang JE, Peired AJ, Chiang EY, Frenette PS. Heterotypic interactions enabled by polarized neutrophil microdomains mediate thromboinflammatory injury. *Nat Med*. 2009; 15(4):384–391.
6. Gross PL, Furie BC, Merrill-Skoloff G, Chou J, Furie B. Leukocyte-versus microparticle-mediated tissue factor transfer during arteriolar thrombus development. *J Leukoc Biol*. 2005;78(6):1318–1326.
7. Wang Y, et al. Leukocyte engagement of platelet glycoprotein Ibalpha via the integrin Mac-1 is critical for the biological response to vascular injury. *Circulation*. 2005;112(19):2993–3000.
8. Simon DI, et al. Platelet glycoprotein ibα is a counterreceptor for the leukocyte integrin Mac-1 (CD11b/CD18). *J Exp Med*. 2000;192(2):193–204.
9. Zarbock A, Polanowska-Grabowska RK, Ley K. Platelet-neutrophil-interactions: linking hemostasis and inflammation. *Blood Rev*. 2007; 21(2):99–111.
10. Hers I, Vincent EE, Tavare JM. Akt signalling in health and disease. *Cell Signal*. 2011;23(10):1515–1527.
11. Yang WL, Wu CY, Wu J, Lin HK. Regulation of Akt signaling activation by ubiquitination. *Cell Cycle*. 2010;9(3):487–497.
12. Woulfe DS. Akt signaling in platelets and thrombosis. *Expert Rev Hematol*. 2010;3(1):81–91.
13. Chen J, De S, Damron DS, Chen WS, Hay N, Byzova TV. Impaired platelet responses to thrombin and collagen in AKT-1-deficient mice. *Blood*. 2004; 104(6):1703–1710.
14. Woulfe D, Jiang H, Morgans A, Monks R, Birnbaum M, Brass LF. Defects in secretion, aggregation, and thrombus formation in platelets from mice lacking Akt2. *J Clin Invest*. 2004;113(3):441–450.
15. O'Brien KA, Stojanovic-Terpo A, Hay N, Du X. An important role for Akt3 in platelet activation and thrombosis. *Blood*. 2011;118(15):4215–4223.
16. Jones CI, et al. A functional genomics approach reveals novel quantitative trait loci associated with platelet signaling pathways. *Blood*. 2009; 114(7):1405–1416.
17. Chen J, Tang H, Hay N, Xu J, Ye RD. Akt isoforms differentially regulate neutrophil functions. *Blood*. 2010;115(21):4237–4246.
18. Di Lorenzo A, Fernandez-Hernando C, Cirino G, Sessa WC. Akt1 is critical for acute inflammation and histamine-mediated vascular leakage. *Proc Natl Acad Sci U S A*. 2009;106(34):14552–14557.
19. Fernandez-Hernando C, et al. Loss of Akt1 leads to severe atherosclerosis and occlusive coronary artery disease. *Cell Metab*. 2007;6(6):446–457.
20. Ding L, et al. Akt3 deficiency in macrophages promotes foam cell formation and atherosclerosis in mice. *Cell Metab*. 2012;15(6):861–872.
21. Barthel SR, et al. Alpha 1,3 fucosyltransferases are master regulators of prostate cancer cell trafficking. *Proc Natl Acad Sci U S A*. 2009;106(46):19491–19496.
22. Zhao Z, et al. Development of potent, allosteric dual Akt1 and Akt2 inhibitors with improved physical properties and cell activity. *Bioorg Med Chem Lett*. 2008;18(1):49–53.
23. Konstantopoulos K, et al. Venous levels of shear support neutrophil-platelet adhesion and neutrophil aggregation in blood via P-selectin and beta2-integrin. *Circulation*. 1998;98(9):873–882.
24. Maugeri N, de Gaetano G, Barbanti M, Donati MB, Cerletti C. Prevention of platelet-polymorphonuclear leukocyte interactions: new clues to the antithrombotic properties of parnaparin, a low molecular weight heparin. *Haematologica*. 2005;90(6):833–839.
25. Evangelista V, et al. Platelet/polymorphonuclear leukocyte interaction in dynamic conditions: evidence of adhesion cascade and cross talk between P-selectin and the beta 2 integrin CD11b/CD18. *Blood*. 1996;88(11):4183–4194.
26. Davenpeck KL, Brummet ME, Hudson SA, Mayer RJ, Bochner BS. Activation of human leukocytes reduces surface P-selectin glycoprotein ligand-1 (PSGL-1, CD162) and adhesion to P-selectin in vitro. *J Immunol*. 2000;165(5):2764–2772.
27. Sengelov H, Kjeldsen L, Diamond MS, Springer TA, Borregaard N. Subcellular localization and dynamics of Mac-1 (alpha m beta 2) in human neutrophils. *J Clin Invest*. 1993;92(3):1467–1476.
28. Ye F, Kim C, Ginsberg MH. Molecular mechanism of inside-out integrin regulation. *J Thromb Haemost*. 2011;9(suppl 1):20–25.
29. Lu Z, Ballou LM, Jiang YP, Cohen IS, Lin RZ. Restoration of defective L-type Ca2+ current in cardiac myocytes of type 2 diabetic db/db mice by Akt and PKC-iota. *J Cardiovasc Pharmacol*. 2011;58(4):439–445.
30. Frenette PS, Atweh GF. Sickle cell disease: old discoveries, new concepts, and future promise. *J Clin Invest*. 2007;117(4):850–858.
31. Paszty C, et al. Transgenic knockout mice with exclusively human sickle hemoglobin and sickle cell disease. *Science*. 1997;278(5339):876–878.
32. Borregaard N, et al. Changes in subcellular localization and surface expression of L-selectin, alkaline phosphatase, and Mac-1 in human neutrophils during stimulation with inflammatory mediators. *J Leuk Biol*. 1994;56(1):80–87.
33. Nanamori M, Chen J, Du X, Ye RD. Regulation of leukocyte degranulation by cGMP-dependent protein kinase and phosphoinositide 3-kinase: potential roles in phosphorylation of target membrane SNARE complex proteins in rat mast cells. *J Immunol*. 2007;178(1):416–427.
34. Servant G, Weiner OD, Herzmark P, Balla T, Sedat JW, Bourne HR. Polarization of chemoattractant receptor signaling during neutrophil chemotaxis. *Science*. 2000;287(5455):1037–1040.
35. Scholz T, Zhao L, Temmler U, Bath P, Heptinstall S, Losche W. The GPIIb/IIIa antagonist eptifibatide markedly potentiates platelet-leukocyte interaction and tissue factor expression following platelet activation in whole blood in vitro. *Platelets*. 2002;13(7):401–406.
36. Caron A, Theoret JF, Mousa SA, Merhi Y. Anti-platelet effects of GPIIb/IIIa and P-selectin antagonism, platelet activation, and binding to neutrophils.

J Cardiovasc Pharmacol. 2002;40(2):296–306.
37. Kleinschnitz C, Pozgajova M, Pham M, Bendszus M, Nieswandt B, Stoll G. Targeting platelets in acute experimental stroke: impact of glycoprotein Ib, VI, and IIb/IIIa blockade on infarct size, functional outcome, and intracranial bleeding. *Circulation*. 2007;115(17):2323–2330.
38. Adams HP Jr, et al. Emergency administration of abciximab for treatment of patients with acute ischemic stroke: results of an international phase III trial: Abciximab in Emergency Treatment of Stroke Trial (AbESTT-II). *Stroke*. 2008;39(1):87–99.
39. Kellert L, et al. Endovascular stroke therapy: tirofiban is associated with risk of fatal intracerebral hemorrhage and poor outcome. *Stroke*. 2013; 44(5):1453–1455.
40. Hahm E, Li J, Kim K, Huh S, Rogelj S, Cho J. Extracellular protein disulfide isomerase regulates ligand-binding activity of alphaMbeta2 integrin and neutrophil recruitment during vascular inflammation. *Blood*. 2013;121(19):3789–3800.
41. Carman CV, Springer TA. Integrin avidity regulation: are changes in affinity and conformation underemphasized? *Curr Opin Cell Biol*. 2003; 15(5):547–556.
42. Moser M, et al. Kindlin-3 is required for β2 integrin-mediated leukocyte adhesion to endothelial cells. *Nat Med*. 2009;15(3):300–305.
43. Lim J, Wiedemann A, Tzircotis G, Monkley SJ, Critchley DR, Caron E. An essential role for talin during alpha(M)beta(2)-mediated phagocytosis. *Mol Biol Cell*. 2007;18(3):976–985.
44. Marchi S, et al. Akt kinase reducing endoplasmic reticulum Ca2+ release protects cells from Ca2+-dependent apoptotic stimuli. *Biochem Biophys Res Commun*. 2008;375(4):501–505.
45. Hogan PG, Lewis RS, Rao A. Molecular basis of calcium signaling in lymphocytes: STIM and ORAI. *Annu Rev Immunol*. 2010;28:491–533.
46. Chang J, Patton JT, Sarkar A, Ernst B, Magnani JL, Frenette PS. GMI-1070, a novel pan-selectin antagonist, reverses acute vascular occlusions in sickle cell mice. *Blood*. 2010;116(10):1779–1786.
47. Cho H, et al. Insulin resistance and a diabetes mellitus-like syndrome in mice lacking the protein kinase Akt2 (PKB beta). *Science*. 2001; 292(5522):1728–1731.
48. Chen WS, et al. Leptin deficiency and beta-cell dysfunction underlie type 2 diabetes in compound Akt knockout mice. *Mol Cell Biol*. 2009; 29(11):3151–3162.
49. Mickelson JK, Lakkis NM, Villarreal-Levy G, Hughes BJ, Smith CW. Leukocyte activation with platelet adhesion after coronary angioplasty: a mechanism for recurrent disease? *J Am Coll Cardiol*. 1996; 28(2):345–353.
50. Chen WS, et al. Growth retardation and increased apoptosis in mice with homozygous disruption of the Akt1 gene. *Genes Dev*. 2001;15(17):2203–2208.
51. Peng XD, et al. Dwarfism, impaired skin development, skeletal muscle atrophy, delayed bone development, and impeded adipogenesis in mice lacking Akt1 and Akt2. *Genes Dev*. 2003;17(11):1352–1365.
52. Ware J, Russell S, Ruggeri ZM. Generation and rescue of a murine model of platelet dysfunction: the Bernard-Soulier syndrome. *Proc Natl Acad Sci U S A*. 2000;97(6):2803–2808.
53. Kim KH, Barazia A, Cho J. Real-time imaging of heterotypic platelet-neutrophil interactions on the activated endothelium during vascular inflammation and thrombus Formation in live mice. *J Vis Exp*. 2013;(74).